Research Journal of Physical Sciences ISSN 2320–4796
Vol. **7(1),** 1-7, January **(2019)** *Res. J. Physical Sci.*

Fractal characteristics in wind speed time series (WSTS) observed at Nalohou (Northern Benin)

Koto N'Gobi G.[1*], Agbazo M.[2], Mamadou O.[1,3], Alamou E.[4], Kounouhéwa B.[1] and Afouda A.[4]
[1]Laboratory of Physics of Radiation (LPR), Abomey-Calavi University, BP: 526 UAC, Bénin
[2]International Chair in Physics Mathematics and Applications (CIPMA-Chair Unesco), Abomey-Calavi University, BP: 526 UAC, Bénin
[3]Institute of Mathematics and Physical Science (IMSP), Abomey-Calavi University, BP: 526 UAC, Bénin
[4]Laboratory of Applied Hydrology (LHA), Abomey-Calavi University, BP: 526 UAC, Bénin
kotgabin36@yahoo.fr

Available online at: www.isca.in, www.isca.me
Received 28th September 2018, revised 15th December 2018, accepted 2nd January 2019

Abstract

Five-years series of thirty minutes average wind speed obtained from AMMA-CATCH stations at Nalohou (Northern Benin), have been analyzed using fractal approach to determine the scaling behavior in wind speed. Wind Speed Time Series (WSTS) have been transferred into an appropriate data form: the fractal-Dimension (Df), and the Critical temporal Scale (Cts) are plotted as function of threshold (Th). Two invariance regimes are obtained in the WSTS. The first regime is defined from 30 min to 32h and the second is from 32 h to 43 days. The fractal Dimensions of these regimes are respectively in [0.2, 1] and [0.6, 1]. The critical temporal scale increases with the increased values of the threshold. Thus, the higher wind intensity can be observed necessary with a larger time scale. The fractal Dimension decreases when the threshold wind speed level increases indicating the presence of multifractal characteristics in the WSTS. This result is confirmed by the $K(q) - q$ *plots function analysis.*

Keywords: Fractal analysis, box counting, wind speed, critical temporal scale, Benin.

Introduction

Energy from wind is one of the worldwide renewable and clean energy which highly depends on wind speed. Wind turbine can produce electricity which extreme instability is caused by little changes in wind speed[1]. Studying wind characteristics in any area is therefore helpful while utilizing energy from wind. Statistics analysis of wind speed and wind frequency are required for the assessment of the energy from wind[2-4]. Also, the intermittency of wind power caused by its temporal and spatial variation is one of the huge challenge to overcome when integrating energy from wind into a local electric grid[5,6]. Benin Republic is one of the West African countries where the available wind power is not clearly known, but one can cite many literatures related to wind studies in this country. Awanou and al.[7] evaluate the mean wind energy available through data from Benin synoptic stations. They found that, the coastal zone is favourable for wind energy than the others regions of the country, far from costal area. Usually, Weibull's function for density of probability is used to estimate wind energy production[8,9]. However, it's shown in Karakasidis[10] et al. and in Jimenez-Hornero et al.[11] that, due to wind speed intermittency over different time scale, the probability density function can't be used efficiently. Fractal theory is one of the best tools used as physical application in several domains of research through the study of fractal Dimension[12,13] (e.g. fractal Dimension in wind study). But fractal theory is less developed in Benin scientific literature as wind time series is concerned. However, analysis of wind speed observations is very challenging for better understanding of its inner dynamical structure for solving future energy problems. According to Haslett and Raftery[14], the analysis of the dynamic in wind speed leads to obtain important informations related to stochastic processes.

For improving scientific knowledge as the temporal structure of wind is concerned in Benin AMMA-CATCH station, we have studied, for the first time, fractal properties of thirty minutes wind speed temporal series. Data analysis and the methodology are presented in the next section. Section 3 presents the results and discussion. Finally, conclusions end the article.

Materials and methods

Site and data description: To reach the goal of the research, we get data from the African Monson Multidisciplinary Analysis (AMMA) network measurements site in Benin (AMMA-CATCH station). We chose thirty minutes automatically recorded wind speed from Nalohou, as available data in the meteorological station located in Djougou from 2008 to 2012. The site is a fallow in a Sudanian climate which annual precipitation (1959-2005) is 1190 mm/year. The mean values of air temperature and relative humidity are respectively ~29°C and ~80%. Sudanian climate is characterized by a single dry season, often starting from October or November to February or March and a single wet season from April to October. The raw time series for wind speed, recorded from 2008 to 2012 is presented on Figure-1. It shows that wind speed varies very strongly during the study period from a low speed value (~ 0.07 $m.s^{-1}$) to a high speed (~ 9 $m.s^{-1}$). The mean wind speed during the study period is 1.3 $m.s^{-1}$.

Methods: Fractal dimension: To describe the non-linear characteristics of observed WSTS, the fractal dimension is explored. The fractal dimension is computed using box counting method[12,14-16]. Let's T be the cumulative time of observation, n the number of disjointed intervals after division of T. Each interval's length is λ. The following values {2^0, 2^1, 2^3…} are attributed to these lengths. The total number of occupied intervals, $N(\lambda)$ (in which at least one WSTS is observed), is:

$$N(\lambda) \propto \lambda^{-D_f} \quad (1)$$

$$\log\big(N(\lambda)\big) = -D_f \, \log(\lambda) + K \quad (2)$$

Where: K is a constant, Df is the Fractal Dimension, opposite value of the slope of the obtained straight line when plotting $log(N(\lambda))$ versus to $log(\lambda)$. The maximum value of Df is equal to one as in litterature[15,16] ($0< Df <1$). The fractal Dimension of each WSTS support is performed at various thresholds, namely: {0, 0.5, 1, 1.5, 2, 2.5 and 3}*M. Where M is the mean value of WSTS concerned.

Trace moment analysis: According to Schertzer and Lovejoy[17], the statistical moments is written as:

$$\langle \phi_\lambda^q \rangle \approx \lambda^{K(q)} \quad (3)$$

ϕ_λ is the field seen at resolution λ, and the moment scaling function $K(q)$ characterizes the multifractal field. Where $\langle . \rangle$ the averaging operator, q is the order of the moment. $\lambda = {L}/{l}$ (Where: L is the largest time scale and l the observation duration). $K(q)$ is the slope of the line obtained by plotting $log(\phi_\lambda^q)$ versus $log\ (\lambda)$. If the log graphs of $K(q)$ versus q is a line, WSTS data present mono-fractal behavior. However, when the curve of log-log diagram of $K(q)$ versus q has a shape of convex function, WSTS have multifractal[18] properties. In this study, q ranges from 0.1 to 3 with step equal to 0.1.

Results and discussion

Fractal dimension: The application of box counting method permit us to draw the Figure-2 on which different intensity of *Th)* are chosen. Seventeen-time resolutions, from (2^0 to 2^{16}) *30 minutes are considered. When *Th* is equal to zero, we obtain a straight line which slope is -1 in the whole scale spectra. This result indicates that, the structure of WSTS is characterized by only one scale invariance with $Df=1$. This suggests the presence of scale invariance in WSTS within this time scale. Three different regimes are obtained when *Th* increases: one with slope equals to -1 (red line) and two (black and blue lines) with *Df*. The two regimes of scale invariance with $Df<1$ named regime 1 and regime 2 are respectively defined between (2^0 to 2^6) *30 minutes and (2^6 to 2^{11}) *30 minutes. With increasing values of *Th*, the curve is composed of three distinctly different sections (Figure-2). From that, WSTS shows scale invariance within a specific interval.

With increasing *Th*, the value of λ at the intersection of straight lines with $Df<1$ and that with $Df =1$ represent the Critical temporal scale, *Cts* as it's found by authors in literature[12] and present currently in Figure-3.

When $\lambda \geq Cts$, so the wind speed exceeding *Th* occurs.

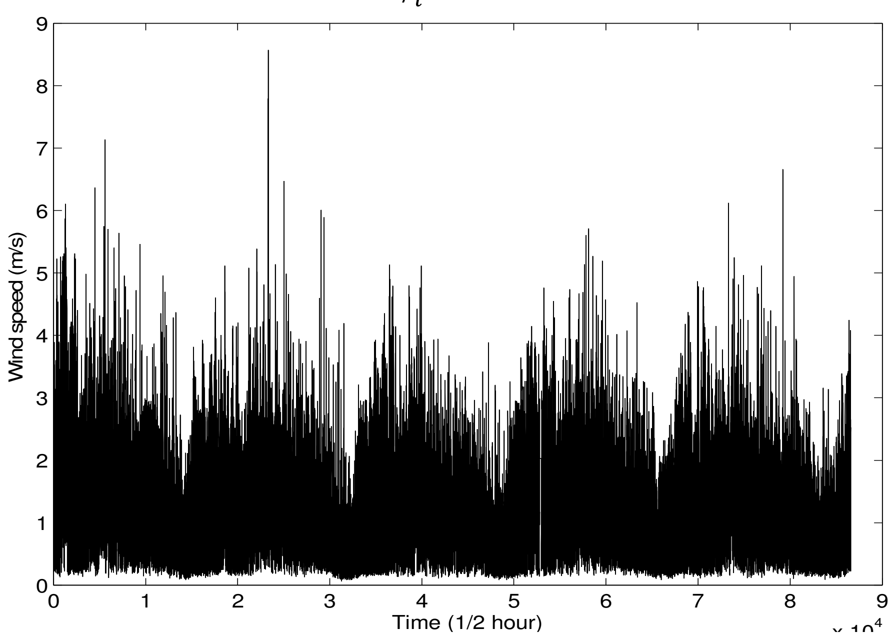

Figure-1: Thirty minutes wind speed data from Nalohou station.

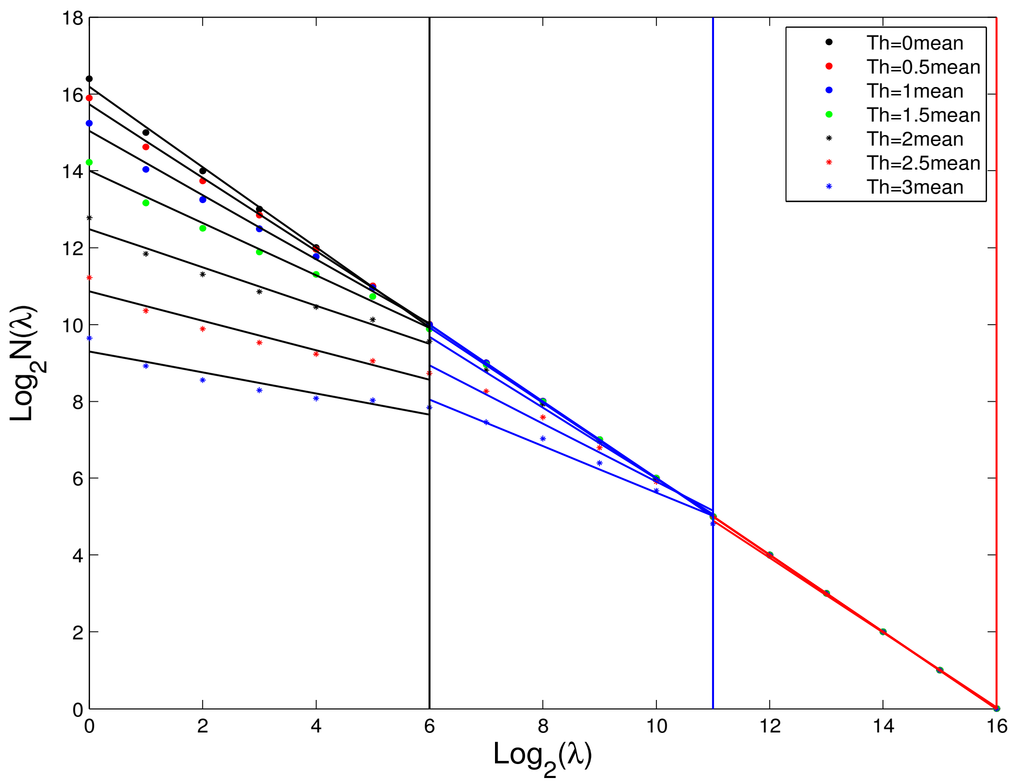

Figure-2: WSTS's $log\ (N(\lambda))$ versus $log\ (\lambda)$ plotting from Box-counting method.

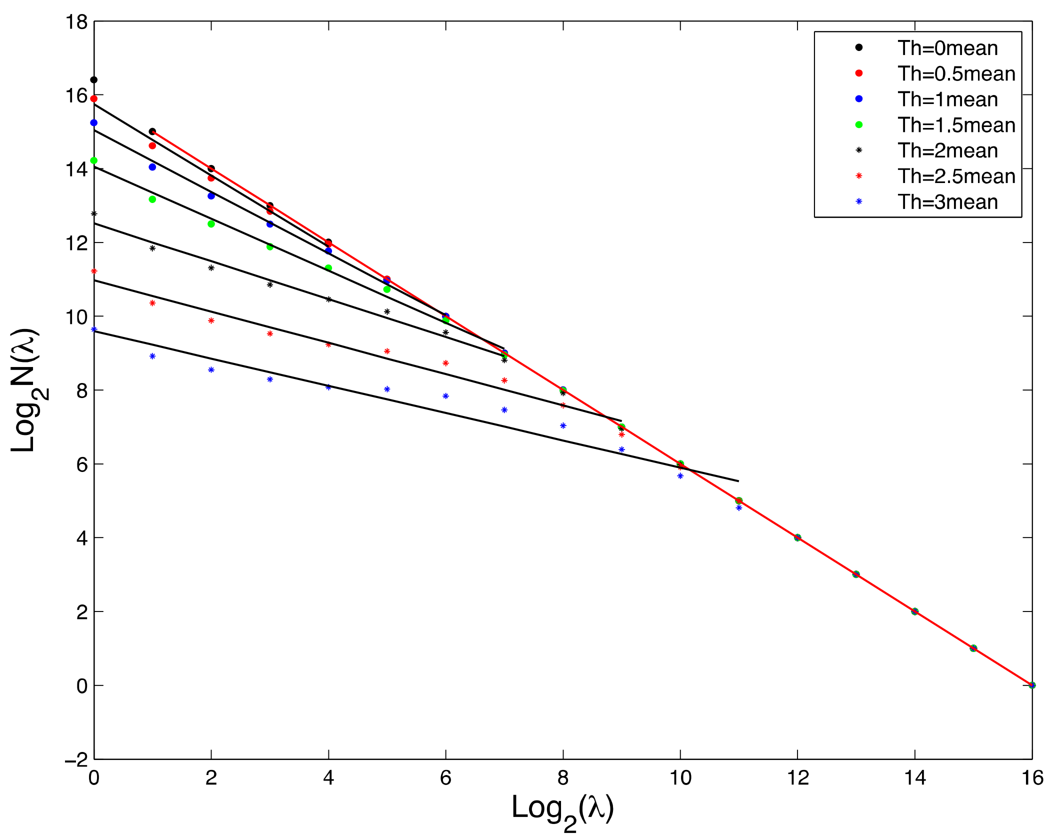

Figure-3: Determination of the Critical temporal scale (*Cts*).

In Figure-4, we present the variation of fractal Dimension obtained over each regime of the scale invariance: regime 1 (in black) and regime 2 (in red) with Threshold.

It is observed that, at the similar *Th*, the fractal dimension of regime 1 are systematically greater than that of regime 2. Figure-4 shows that *Df* decreases as Th increases. This implies that the WSTS properties varies with the threshold. At low values of *Th* (0-1.5*M), the curves of second regime decreases slowly. For low wind speed in regime 2, WSTS structure is more discrete so that the persistence of the intermittence is less continuous than in the regime 1. Figure-5 shows the variation of Critical temporal scale (*Cts*) with threshold.

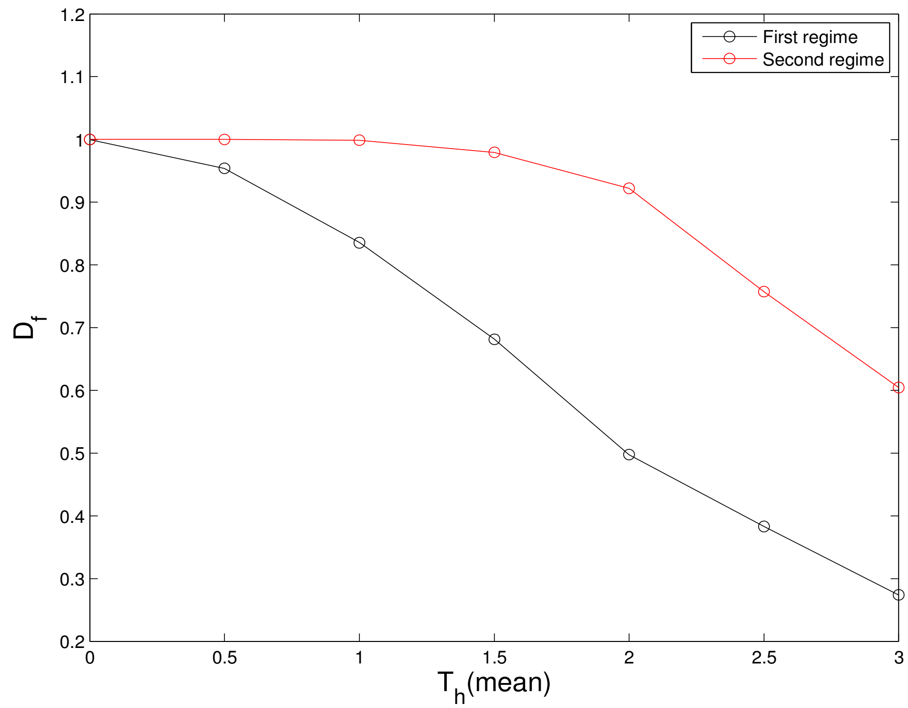

Figure-4: *Df- Th* plot, obtained over each regime of the scale invariance, regime 1 (black) and regime 2 (red).

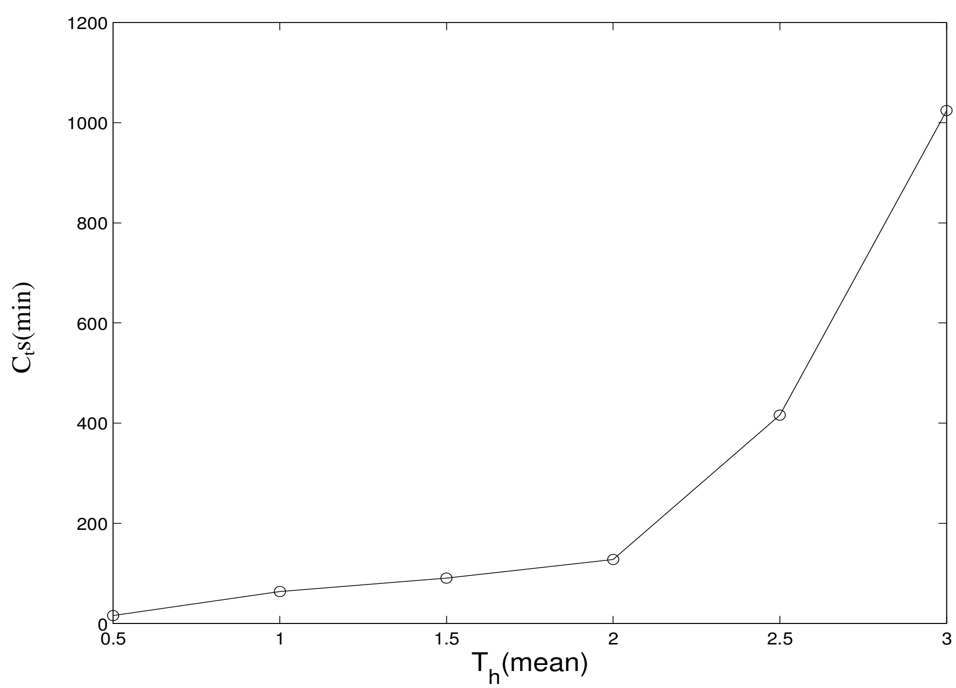

Figure-5: *Cts-Th* plot of Wind speed time series.

Cts increases with *Th* values. It means that, wind intensity can be observed necessary with a larger time scale. *Df-Th* and *Cts-Th* plots have the same meaning. For certain values of *Th*, a sparser time structure can be produced with larger values of Critical temporal Scale, and inversely. Thus, some temporal characteristics in WSTS can be determined analysing both *Df-Th* and *Cts-Th* plots.

Finally, the results from the monofractal study shown above is not sufficient for describing the scaling characteristics of WSTS. So, the Cts values increase with *Th* as it's shown by C.K. Lee[13]. Our results, as Lee's[13], mean that different scaling properties of WSTS are observed with different *Th* intensities[13]. Thus, a multifractal structure could be used to describe the WSTS.

Multifractal scaling analysis: Figure-6 shows *log–log* plot of the *q*-order moments $\langle R_\lambda^q \rangle$ versus the resolution λ, q varies from 0.1 to 3.0 with step equal to 0.1.

Straight lines in Figure-6 reveal the scaling behavior of WSTS from 30 minutes to 43 days. In Nalohou, Trace Moment analysis show that thirty wind speed presents one scaling regime defined between 30 minutes and 43 days. Figure-7 is the chart of *K(q)* describing the scale of the statistical moments from 30 minutes to 43 days.

The shape of *K(q)* is convex, indicating that WSTS is multifractal. This result confirms the precedent fractal analysis. Our result of the Wind Speed Time Series is grate because it could have important potential in modeling the wind speed structure.

Conclusion

This study aims to investigate fractal characteristics of 30 minutes WSTS recorded at Nalohou (Northern Benin) from 2008-2012 by applying box counting and Trace Moment methods. The found results can be summarise as: i. monofractal analysis is not sufficient for describing the scaling properties of WSTS in the study region, ii. the values of fractal Dimension decrease as the threshold values increase, indicating that different scaling behavior are observed with changing in threshold values. Therefore, multifractal theory is adapted to analyse the studied wind speed time series, iii. WSTS displays scale invariance through a specific time interval, and iv. wind speed shows stronger multifractality behavior on the scaling regime defined between 30 minutes and 43 days.

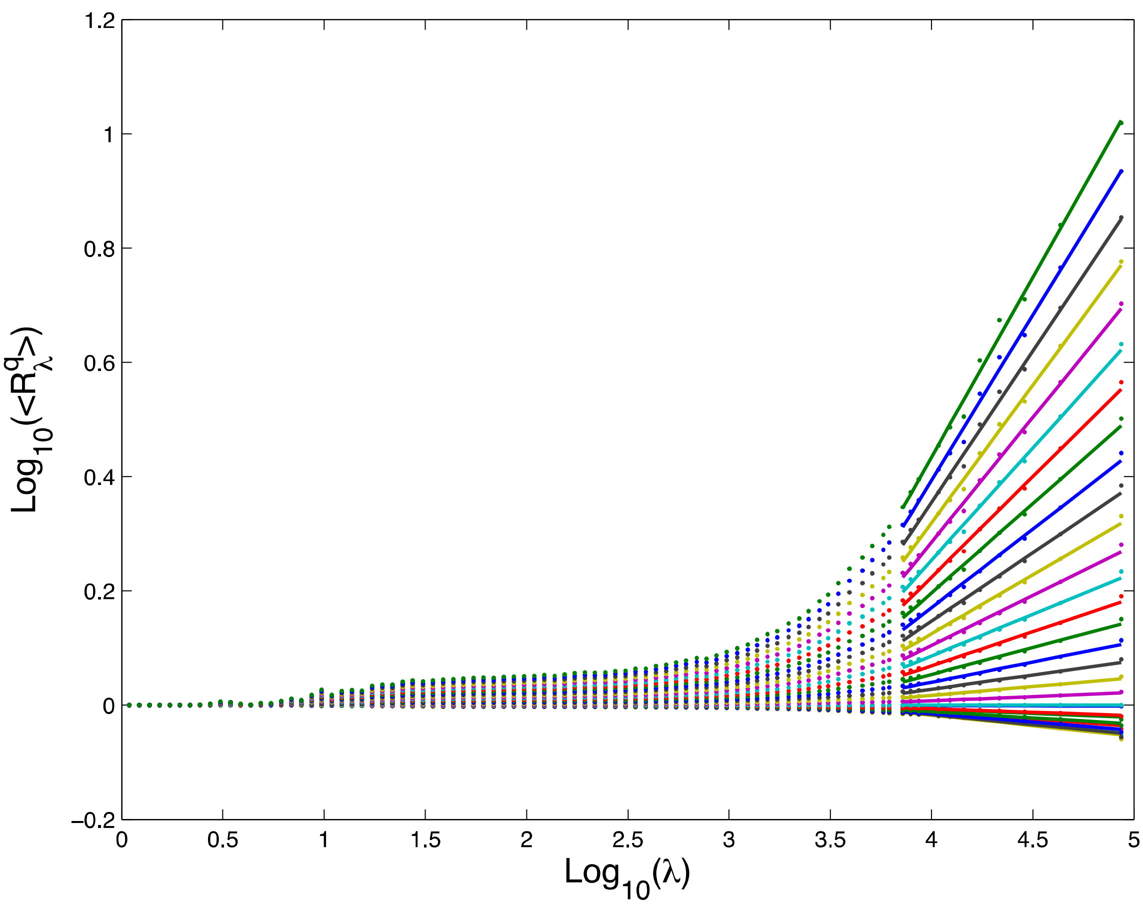

Figure-6: *log*($\langle R_\lambda^q \rangle$) versus *log*($\lambda$). From top to bottom *q* ranges from 0.1 to 3.0 with step equal to 0.1.

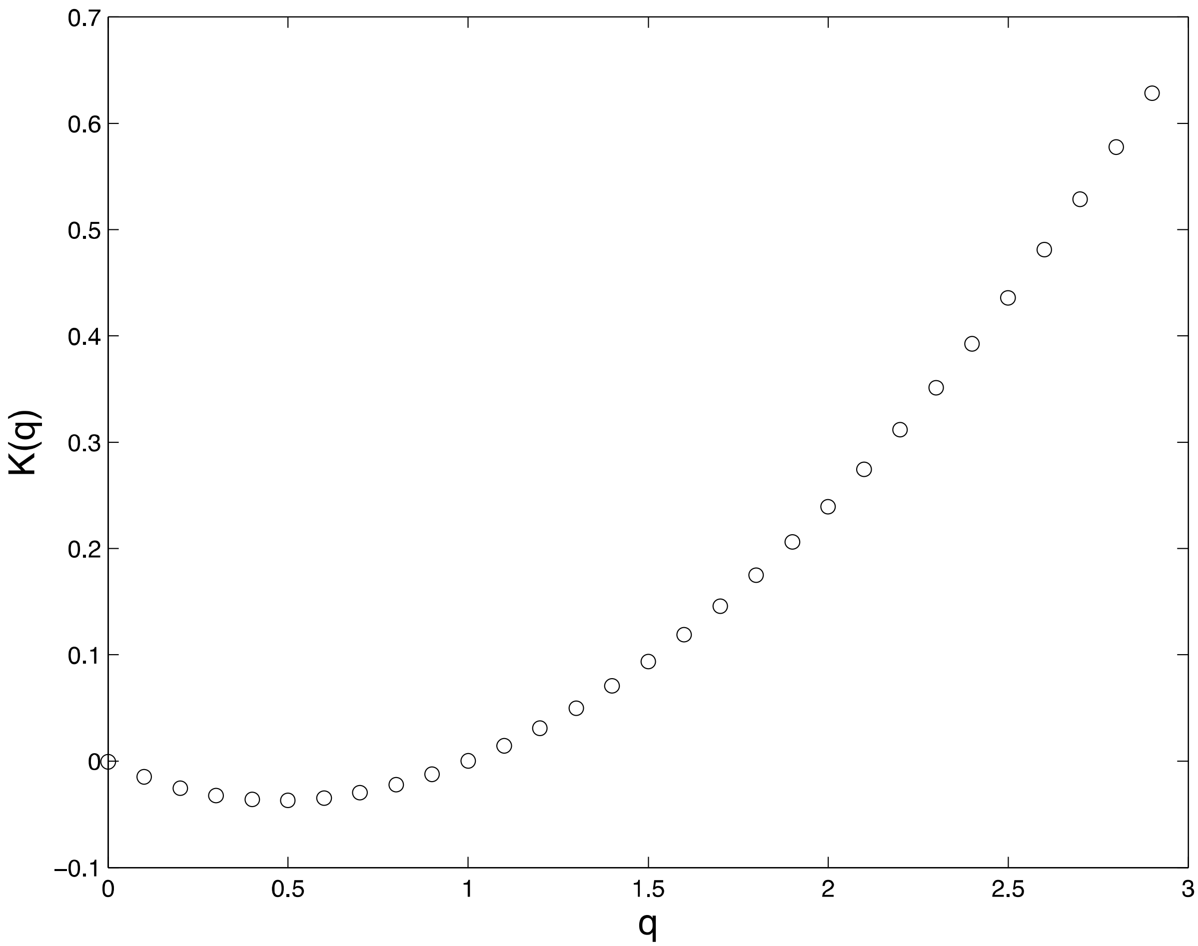

Figure-7: Empirical moment scaling exponent function *K(q)*.

Acknowledgments

All the authors would like to thank AMMA–CATCH project IRD, INSU to have funded the installation of Nalohou station, from where the data was provided. We also thank, "Direction Générale de l'Eau (DG-Eau)", Benin.

References

1. Chang T.P., Ko H., Liu F.J., Chen P.H., Chang Y.P., Liang Y.H., Jang H.Y., Lin T.C. and Chen Y.H. (2012). Fractal dimension of wind speed time series. *Applied Energy*, 93, 742-749.
2. de Araujo Lima L. and Bezerra Filho C.R. (2010). Wind energy assessment and wind farm simulation in Triunfo–Pernambuco, Brazil. *Renewable Energy*, 35(12), 2705-2713.
3. Pimenta F., Kempton W. and Garvine R. (2008). Combining meteorological stations and satellite data to evaluate the offshore wind power resource of Southeastern Brazil. *Renewable Energy*, 33(11), 2375-2387.
4. Shipkovs P., Bezrukov V., Pugachev V., Bezrukovs V. and Silutins V. (2013). Research of the wind energy resource distribution in the Baltic region. *Renewable Energy*, 49, 119-123.
5. Leahy P.G. and Mckeogh E.J. (2013). Persistence of low wind speed conditions and implications for wind power variability. *Wind Energy*, 16(4), 575-586.
6. Bakker A.M.R. and Van Den Hurk B.J.J.M. (2012). Estimation of persistence and trends in geostrophic wind speed for the assessment of wind supply in Northwest Europe. *Climate Dynamics*, 39(3-4), 767-782.
7. Awanou C.N., Degbey J.M. and Ahlonsou E. (1991). Estimation of the mean wind energy available in Benin (Ex Dahomey). *Renewable Energy*, 1(5-6), 845-853.
8. Houekpoheha M.A., Kounouhéwa B., Tokpohozin B.N. and Awanou C.N. (2014). Estimation de la puissance énergétique éolienne à partir de la distribution de Weibull sur la côte béninoise à Cotonou dans le Golfe de Guinée. *Revue des Energies Renouvelables,* 17(3), 489-495.
9. Akpo A.B., Damada J.C.T., Donnou H.E.V., Kounouhewa B. and Awanou C.N. (2015). Evaluation de la production

énergétique d'un aérogénérateur sur un site isolé dans la région côtière du Bénin. *Revue des Energies Renouvelables*, 18(3), 457-468.

10. Karakasidis T.E. and Charakopoulos A. (2009). Detection of low-dimensional chaos in wind time series. *Chaos, Solitons & Fractals*, 41(4), 1723-1732.

11. Jiménez-Hornero F.J., Pavón-Domínguez P., de Ravé E.G. and Ariza-Villaverde A.B. (2011). Joint multifractal description of the relationship between wind patterns and land surface air temperature. *Atmospheric Research*, 99(3-4), 366-376.

12. Lee C.K., Juang L.C., Wang C.C., Liao Y.Y., Yu C.C., Liu Y.C. and Ho D.S. (2006). Scaling characteristics in ozone concentration time series (OCTS). *Chemosphere*, 62(6), 934-946.

13. Lee C.K., Ho D.S., Yu C.C. and Wang C.C. (2003). Fractal analysis of temporal variation of air pollutant concentration by box counting. *Environmental Modelling and Software*, 18(3), 243-251.

14. Haslett J. and Raftery A.E. (1989). Space-time modeling with long-memory dependence: assessing Ireland's wind power resource. *Applied Statistics*, 38, 1-50.

15. Mandelbrot B.B. (1983). The Fractal Geometry of Nature. W.H. Freeman and Company, New York, 468.

16. Lovejoy S.D.A.A., Schertzer D. and Tsonis A.A. (1987). Functional box-counting and multiple elliptical dimensions in rain. *Science*, 235(4792), 1036-1038.

17. Hubert P. and Carbonnel J.P. (1989). Dimensions fractales de l'occurrence de ploy en climat soudano-sahélien. *Hydrologie Continentale*, 4(1), 3-10.

18. Biaou A. (2004). De la méso-échelle à la micro-échelle: Désagrégation spatio-temporelle multifractale des précipitations. Thèse de doctorat, Ecole de Mines de Paris, France.

19. Hoang C.T. (2011). Prise en compte des fluctuations spatio-temporelles pluies-débits pour une meilleure gestion de la ressource en eau et une meilleure évaluation des risques. *Sciences de la Terre*, Université Paris-Est.

20. Lovejoy S. and Schertzer D. (1990). Multifractals, universality classes and satellite and radar measurements of cloud and rain fields. *J Geophys Res*, 95, 2021-2034.

21. Parisi G. and Frisch U. (1985). Multifractal model of intermittency, in turbulence and predictability. *geophysical fluid dynamics and climate dynamics, North Holland*: 84-88.